Publishing House
AKAPIT

COMPUTER METHODS IN MATERIALS SCIENCE

Informatyka w Technologii Materiałów

Vol. 17, 2017, No. 4

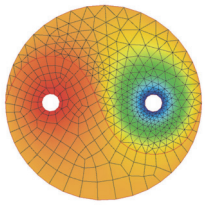

NUMERICAL MODEL OF COLD DEFORMATION OF TRIP STEEL

ŁUKASZ RAUCH[1], MARIUSZ SKÓRA[2], KRZYSZTOF BZOWSKI[1]*, MACIEJ PIETRZYK[1]

[1] AGH University of Science and Technology, al. Mickiewicza 30, 30-059 Kraków, Poland
[2] GAWEL Zakład Produkcji Śrub S.A., 36-073 Strażów, Poland
**Corresponding author: kbzowski@agh.edu.pl*

Abstract

Exploring possibilities of modelling deformation of TRIP steel during manufacturing of fasteners was the objective of the paper. Homogenised flow stress model for the investigated steels was determined first on the basis of compression tests. Inverse analysis was applied to eliminate the effect of friction and deformation heating in compression. Possibility of prediction of local strains and stresses accounting for the TRIP effect was investigated next. Representative Volume Element (RVE) and Statistically Similar Representative Volume Element (SSRVE) with TRIP microstructures were developed and subjected to deformation. Transformation of the retained austenite into martensite was simulated. Computing costs of the RVE and SSRVE were compared and it was shown that they are an order of the magnitude lower for the latter. The SSRVE based micro model, which can be attached to the FE code which simulates forging of fasteners, is the main output of the paper.

Key words: plastic deformation, fasteners, TRIP effect; material model, Representative Volume Element

1. INTRODUCTION

A long-standing ambition for steel product manufacturers has been to develop a class of steels where both ductility and strength can be simultaneously improved. This improvement in modern carbon steels is obtained by a combination of soft ferrite with hard constituents like bainite, martensite and retained austenite (Kuziak et al., 2008). In this group of steels, transformation-induced plasticity TRIP-assisted steels are particularly appealing. TRIP steels are a class of multiphase steels that exhibit a good combination of strength and ductility. This unique characteristic is attributed to the presence of a metastable retained austenite (RA) in the microstructure at room temperature. Upon applied thermal and/or mechanical loadings, the retained austenite may transform into a harder martensitic phase, which may increase the effective strength of the material. In addition, transformation from austenite to martensite is accompanied by shape and volume changes, which are accommodated by local plastic deformations in the surrounding phases, creating the so-called "TRIP-effect" (Iwamoto, 2008; Davut, 2013). The additional plastic deformation due to the transformation increases the effective work-hardening of the material. In comparison to similar steels that contain no retained austenite in their microstructure, e.g., dual-phase (DP) steels, TRIP steels have a similar ultimate strength, but exhibit a significantly higher ductility.

Problem of deformation of TRIP steels has been thoroughly researched during last two decades. Perlade et al. (2003) proposed mean field physically based model for TRIP-aided carbon steels. Advanced mechanical models were created by Perdahcioglu and Geijselaers (2015). Authors of (Papatriantafillou et al., 2004) treated TRIP steels as composite materials with a ferritic matrix containing bainite and retained austenite, which gradually transforms into martensite. The effective properties and overall behaviour of TRIP steels are determined by

ISSN 1641-8581

using homogenization techniques for non-linear composites. Homogeneization was applied to develop a methodology for the numerical integration of the resulting elastoplastic constitutive equations in the finite element (FE) method. Problem of coupling between plasticity and martensitic phase transformation has been treated by Cherkaoui (2000). Many more papers dealing with deformation of TRIP steels and TRIP effect were published and comprehensive review was done in (Fonstein, 2015). The objectives of the present paper were formulated having in mind a model with prospective application to industrial forging process of fasteners. These objectives were twofold. The first was identification of the conventional model with coefficients determined on the basis of compression tests performed on Gleeble 3800. This model was applied in simulations of primary forming processes in the manufacturing chain. The second objective was development of the micro model of the TRIP effect, using SSRVE (Statistically Similar Representative Volume Element) approach (Schroeder et al., 2011). This model when attached to the FE code will have capability to predict local properties (hardness) accounting for the TRIP effect. In the present paper an attempt was made to develop SSRVE for the TRIP steel using the methodology, which was successfully applied by Rauch et al. (2011) to represent Dual Phase (DP) microstructure. It appeared that the quality of the micrographs was not satisfactory to distinguish and reproduce unambiguously ferrite, bainite, retained austenite and martensite. Therefore, artificial generation method was used in the present paper to develop SSRVE for a TRIP steel.

2. LOW-ALLOYED TRIP STEELS

The term ”TRIP steel” actually covers a wide range of steels containing a meta-stable austenite phase, which can be present in room temperature microstructure of both high and low alloyed steels (Davut, 2013; Fonstein, 2015). Typical microstructure of an undeformed low-alloyed TRIP steel is composed of ferrite, bainite, metastable retained austenite and potentially martensite. Intercritical ferrite is the most dominant phase since it occupies up to 80% of the microstructure. Ferrite has a body-centred cubic (BCC) lattice and it is the softest phase among the constituent phases. The size of ferrite grains in a typical TRIP steel is in the range of 5 − 10 μm (Furnemont et al., 2002). Unlike ferrite, a typical bainite is not a single-phase constituent and it consists of fine platelets of ferrite that form and cementite (Fe3C) that precipitates in-between and/or inside the ferrite platelets. In general, bainite is harder than intercritical ferrite due to its finer structure as well as the presence of carbide precipitations. Due to presence of the silicon, the bainite in TRIP steels is essentially carbide-free and is referred to as ”bainitic ferrite”, which is not exactly the same as the typical bainite (Bhadeshia and Christian, 1990). Mechanisms contributing to development of the microstructure in the Si-containing bainitic steels are described well by Guo et al. (2017). In the present paper in the SSRVE bainite is treated as an uniform phase with homogenized properties.

Retained austenite is the key constituent of the TRIP steel microstructure. It is a meta-stable phase at room temperature. Carbon enrichment and the constraining effect from neighbouring grains stabilize austenite at room temperature. Due to the strengthening effect of carbon, the strength of retained austenite in TRIP steels is generally higher than that of the ferrite. Occasionally, the initial TRIP steel microstructure can contain a small fraction of martensite, that forms when the austenite is rapidly cooled.

As it has been mentioned in the introduction, the unique mechanical properties of TRIP steels are attributed mainly to the presence of the metastable retained austenite phase in the room temperature microstructure. During deformation the retained austenite can transform into a harder martensite, which would increase the effective strength of the material. The plastic strain appears first in the soft phase and the harder phase can maintain its ductility until the later stages of overall deformation. Reproducing these phenomena in the SSRVE was one of the objective of the present paper.

3. EXPERIMENT

Experiments were performed on the Gleeble 3800 thermomechanical simulator in the Institute for Ferrous Metallurgy in Gliwice. Two steels with chemical composition in Table 1 were tested. Difference between the steels was mainly in the silicon content. Each steel was prepared in the form of laboratory heat (marked L in the paper) and in the form of samples taken from the production (marked P in the paper). The samples measuring ϕ5×7 mm were deformed at temperatures 20, 100, 200 and 300^{o}C and at strain rates 0.1, 1 and 10, s^{-1}. The total strain measured as the height reduction was $\varepsilon = 1$ (ε

$= \ln(h_1/h_2)$, where h_1, h_2 – height of the sample before and after the test). Load vs. displacement data were monitored at each test. Beyond this, surface temperature of the sample was measured. Selected examples of the registered loads are shown in Fig. 1. It is seen in this figure that the effects of strain rate and temperature are small. Beyond this the strain rate sensitivity is reverse, the loads decrease with increasing strain rate. Fig. 2 shows comparison of loads measured for various steels. These plots show that differences between various materials are negligible. The results for the strain rate of 0.1 s^{-1} only are presented but similar results were obtained for other strain rates.

Table 1. *Chemical composition of the investigated steels, wt%.*

Steel	C	Mn	Si	P	S	Cr
A	0.08	1.44	0.847	0.008	0.019	0.03
B	0.18	1.39	0.228	0.011	0.008	0.03

4. INVERSE ANALYSIS

Inverse analysis was used to determine the real flow stress corrected against the effect of friction and deformation heating in the plastometric tests. The latter is particularly important, what is confirmed by plots in figure 3, where measurements of the temperature are shown. It is seen that in fast tests an increase of the temperature exceeds 100°C.

The inverse algorithm proposed by Szeliga et al. (2006) and described in detail in (Pietrzyk et al., 2015) was used. The flow stress values corresponding to the subsequent strains were determined using optimization techniques. The quadratic norm of the error between measured and calculated compression loads was used as the objective function:

$$\Phi = \sqrt{\frac{1}{Nt}\sum_{i=1}^{Nt}\left[\frac{1}{Ns}\sum_{j=1}^{Ns}\left(\frac{F_{ij}^{m}-F_{ij}^{c}}{F_{ij}^{m}}\right)^{2}\right]} \qquad (1)$$

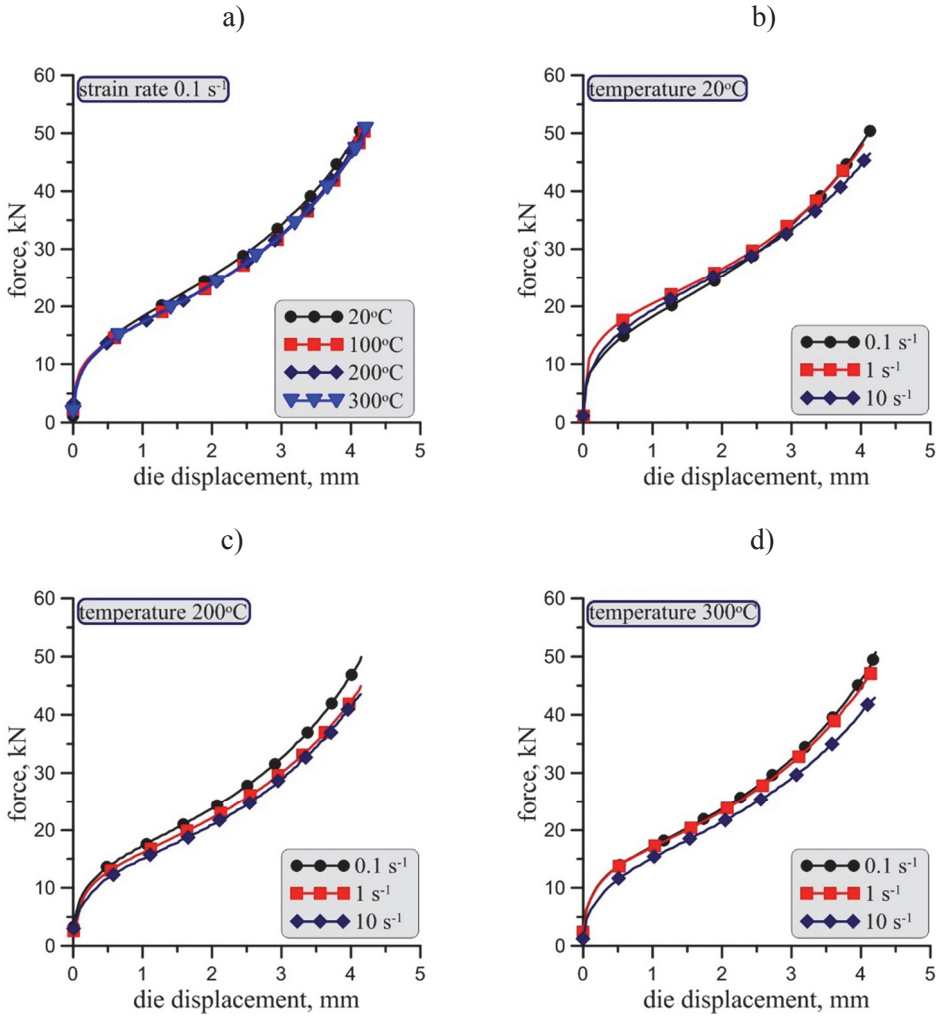

Fig. 1. *Selected example of the registered loads for the laboratory heat (L) of the steel A, strain rate 0.1 s^{-1} (a) and different temperatures: 20°C (b), 200°C (c) and 300°C (d) and different strain rates.*

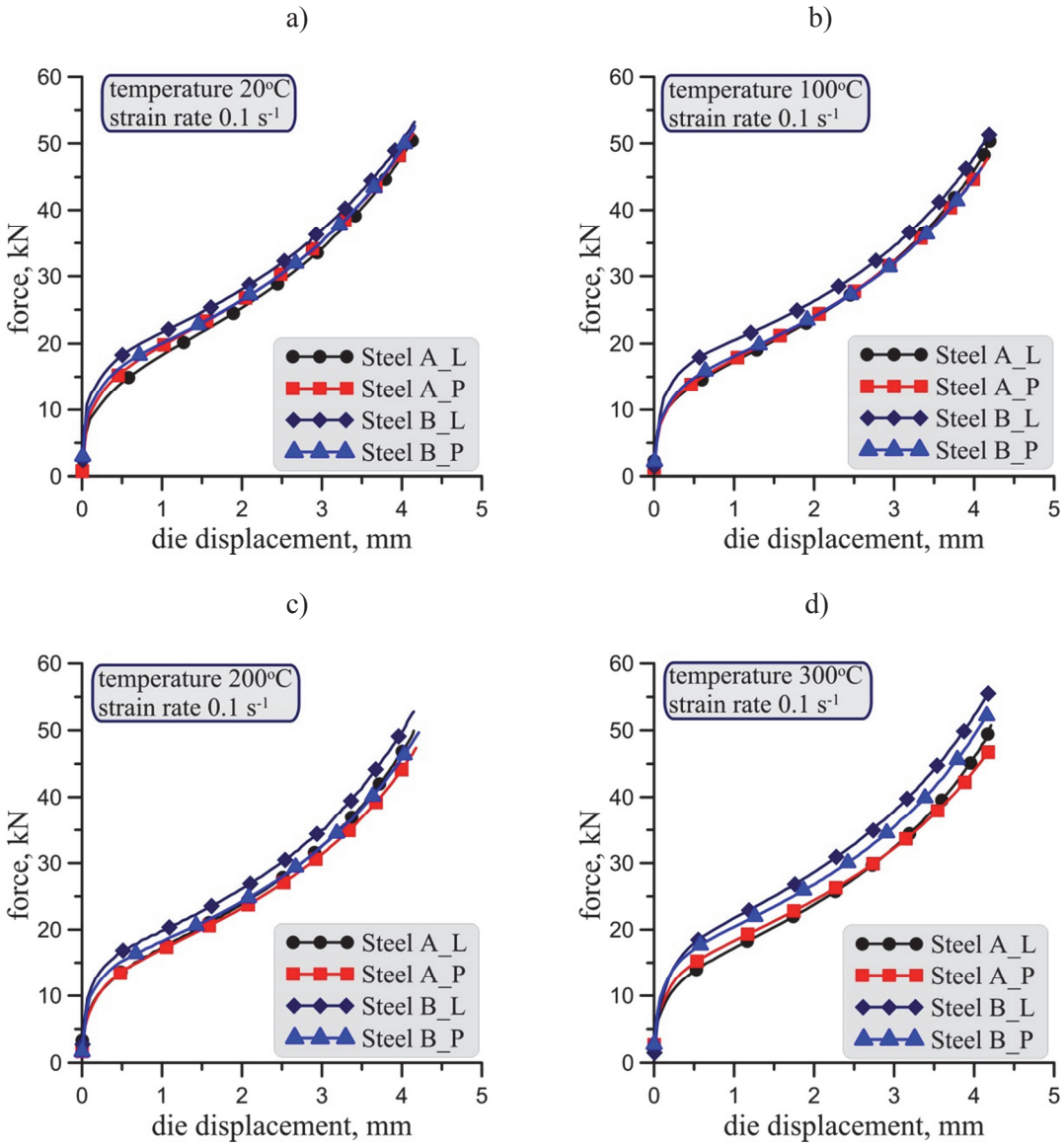

Fig. 2. *Selected examples of comparison of the registered loads for steels A and B at various states, strain rate 0.1 s^{-1} and different temperatures.*

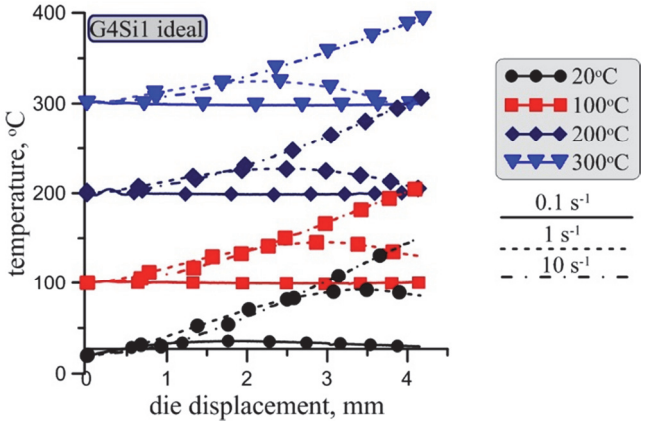

Fig. 3. *Temperatures measured during the tests.*

where: F_{ij}^{m}, F_{ij}^{c} – measured and calculated load, Nt – number of tests, Ns – number of load measurement sampling points in one test, Φ – quadratic norm of the error. For each iteration of the optimization procedure: coefficients of the flow curve equations were adjusted, simulation was performed and calculated compression loads were compared with the experimental values.

Due to the influence of friction and deformation heating application of the inverse analysis of the plastometric tests is an inevitable condition of obtaining realistic flow stress data. Selected results of the analysis for the laboratory heat of the steel A are shown in figure 4. The curves in this figure represent flow stress as a function of true strain, which were obtained in a tabular form. This relation can be considered a property of material for isothermal, constant strain rate conditions. The obtained functions introduced in the finite element program together with correction for variations of temperature and strain rate will give perfect agreement between measured and predicted loads.

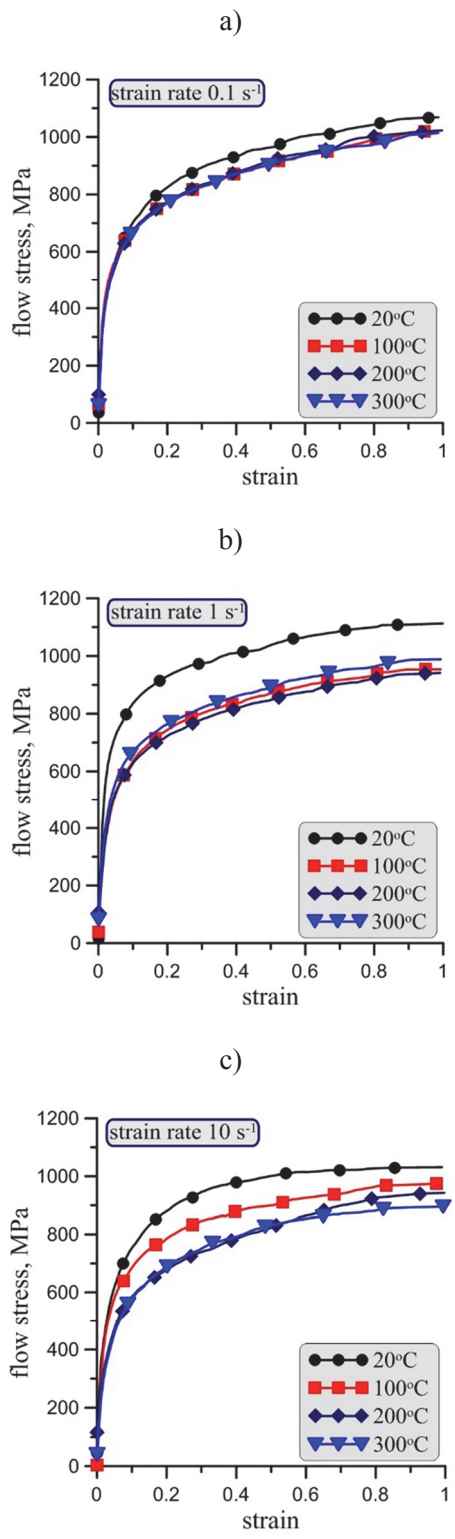

Fig. 4. *Flow stress as a function of true strain for the laboratory heat of the steel A, true strain rates 0.1 s^{-1} (a), 1 s^{-1} (b) and 10 s^{-1} (c).*

The same results presented for one temperature and different true strain rates are shown in figure 5. Analysis of all results sows that the flow stress decreases noticeably when temperature increases from the room temperature to 100°C. Further increase of the temperature has small effect. Influence of the strain rate is negligible and inconsistent. Therefore, the second part of the inverse analysis was performed and coefficients in the equation describing the flow stress were the design variables in the optimization.

The equation proposed by Hensel-Spittel (1970) was used as the flow stress model:

$$\sigma_p = \alpha\varepsilon^n \exp(q\varepsilon)\dot{\varepsilon}^m \exp(-\beta T) \qquad (2)$$

where: ε – effective true strain, T – temperature in °C, α, n, q, m, β - coefficients, which were determined using the inverse analysis.

For the laboratory heat of the steel A the optimization yielded the following valued of coefficients: $\alpha = 1108$, $n = 0.193$, $q = 0$, $m = 0$, $\beta = 0.0000437$. Inverse analysis for the remaining steels showed that only coefficient A changed slightly and the following values were obtained: for the production samples of the steel A $\alpha = 1063.7$, for the laboratory heat of the steel B $\alpha = 1227.3$ and for the production samples of the steel B $\alpha = 1194.4$. These coefficients mean that on average, the materials does not show strain rate sensitivity and very weak dependence on the temperature. Equation (2) with optimal coefficient could be used in the FE simulation of the primary forming processes in the manufacturing chain. Since plots of the flow stress calculated from equation (2) with optimal coefficients coincide with the plots obtained in the tabular form from the first step of the inverse analysis, they are not shown in the paper.

5. RVE AND SSRVE

5.1. Representation of the TRIP microstructure

Using microstructure in calculations in explicit way is always computationally costly due to the necessity of applying very fine mesh to obtain reliable discretization of the surface. This is a reason why often Representative Volume Elements (RVE) are used. An usual RVE is determined by the smallest possible sub domain, which is still able to represent the macroscopic behaviour of the material. In the micro-macro modelling approach a RVE representing the underlying microstructure is attached at each Gauss point of the macroscopic solution. The constitutive law describing material behaviour in the macroscale is obtained by averaging the first Piola-Kirchoff stresses with respect to the RVE.

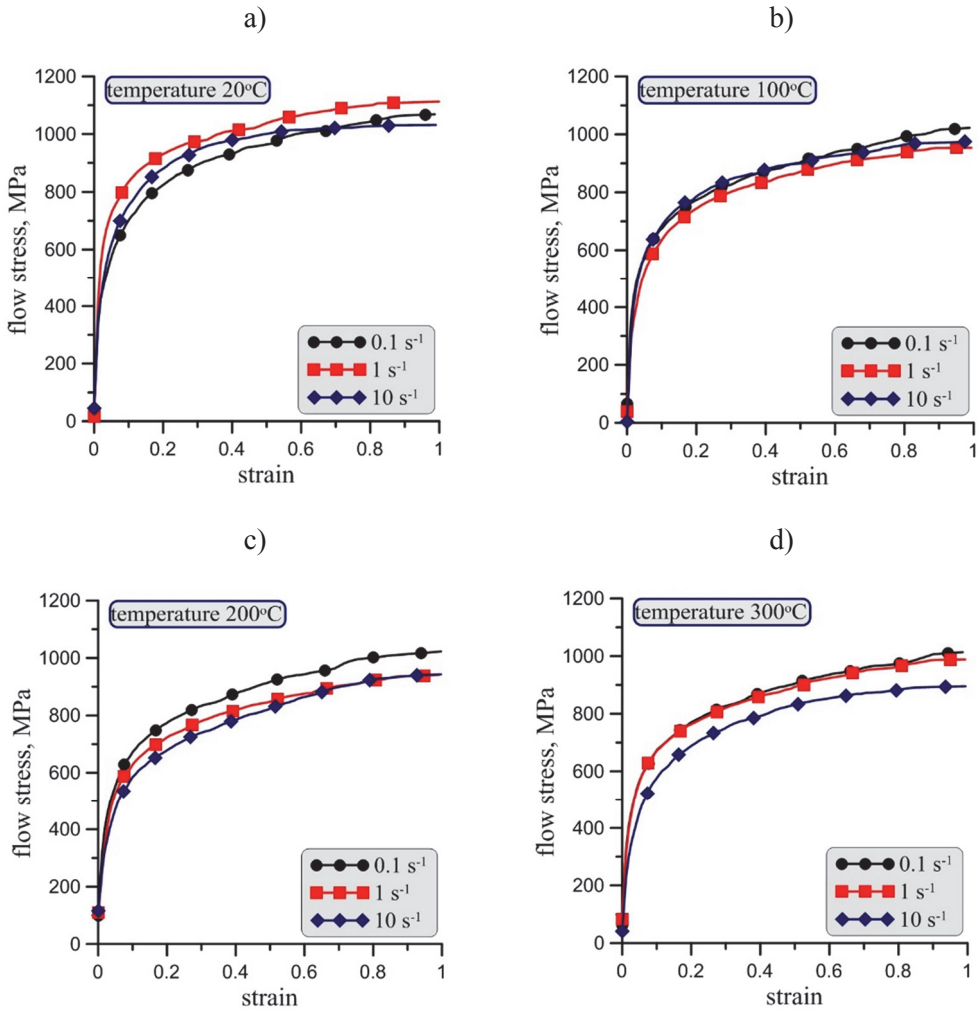

Fig. 5. *Flow stress as a function of true strain for the laboratory heats of the steel A at 20°C (a), 100°C (b), 200°C (c), 300°C (d), and true strain rates 0.1 s^{-1}, 1 s^{-1} and 10 s^{-1}.*

Analysis of the computing costs showed that that RVE simulations with the TRIP effect are still not effective. Although the RVEs are the smallest possible by a definition, they still can be too complex for the efficient calculations, in particular when multiscale approach is applied. Therefore, the construction of statistically similar RVE (SSRVE), which is characterized by a lower complexity than the smallest possible substructure, was proposed as a second alternative in this paper.

The theoretical basis of the micro-macro modelling is well described in the scientific literature, e.g. (Schroder et al., 2011) and it is not repeated here. The focus is on the development of the simple SSRVE, which will allow to decrease the computing costs and will make micro-macro modelling approach more efficient.

5.2. Construction of the SSRVE

Schematic illustration of the TRIP steel microstructure is shown in Fig. 6a.The basic idea of the SSRVE is to replace a RVE with an arbitrary complex inclusion morphology by a periodic one composed of optimal unit cells. This idea was proposed by Schroeder et al. (2011). Authors of the present paper developed an algorithm based on shape coefficients described in (Rauch et al., 2011), where it was used to the analysis of the DP steel microstructures. The parameters, describing fraction of different phases and their geometrical characteristics, which form a group of the most important parameters, were applied by Rauch et al. (2011). An attempt to use this approach for the TRIP steels was made in the present paper but due to not satisfactory quality of micrographs the results were unambiguous. Therefore, in order to test and validate the micro model, SSRVE was generated artificially for the typical phase composition of the TRIP steel containing ferrite (~40%), bainite (~40%), martensite (~10%) and residual austenite (~10%), as shown schematically in Fig. 6b.The volume fractions of phases were the only criterion in optimization. This SSRVE was subjected to deformation in compression.

a)

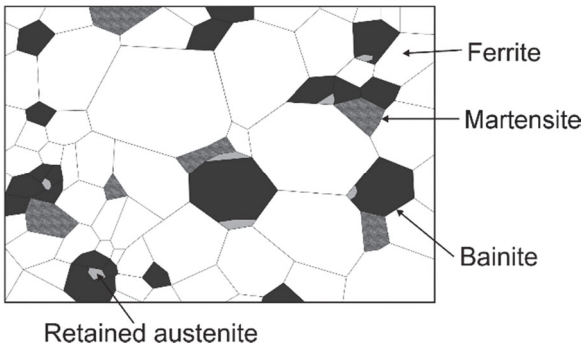

b)

Fig. 6. Schematic illustration of the TRIP steel microstructure (a) and artificially generated SSRVE.

5.3. Deformation

Before forging hot rolled steel rods are subjected to cold drawing first. The objective is to improve surface quality and to reduce variations of the diameter. Macro scale simulations of the drawing process were performed using finite element (FE) method and SSRVE representing TRIP microstructure was attached to the flow lines in the deformation zone, as it is shown by Konstantinov et al. (2015). An image of the TRIP microstructure shown in Fig. 6b was used to perform the micro scale simulation. A binarized image of the microstructure was covered with a FE mesh with 12000 linear quadrilateral elements using Abaqus standard library. 10% displacement boundary condition was applied on a top tool part. Position of bottom tool was fixed entire whole simulation. Frictionless mechanical contact between artificial tools and microstructure was used. The rheological model was elastoplastic. Flow stress curves for the phase components proposed by Papatriantafillou (2005) are presented in figure 7.

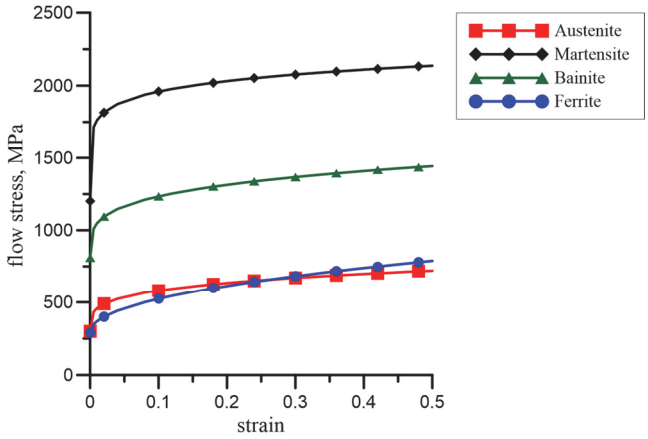

Fig. 7. Flow curves for phase components.

a)

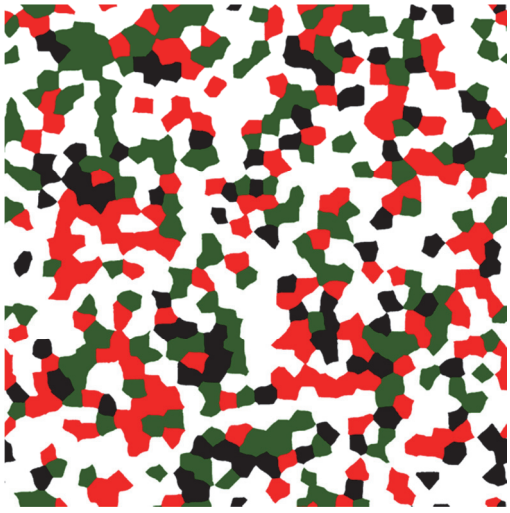

b)

Fig. 8. RVE (a) and SSRVE (b) with TRIP microstructure.

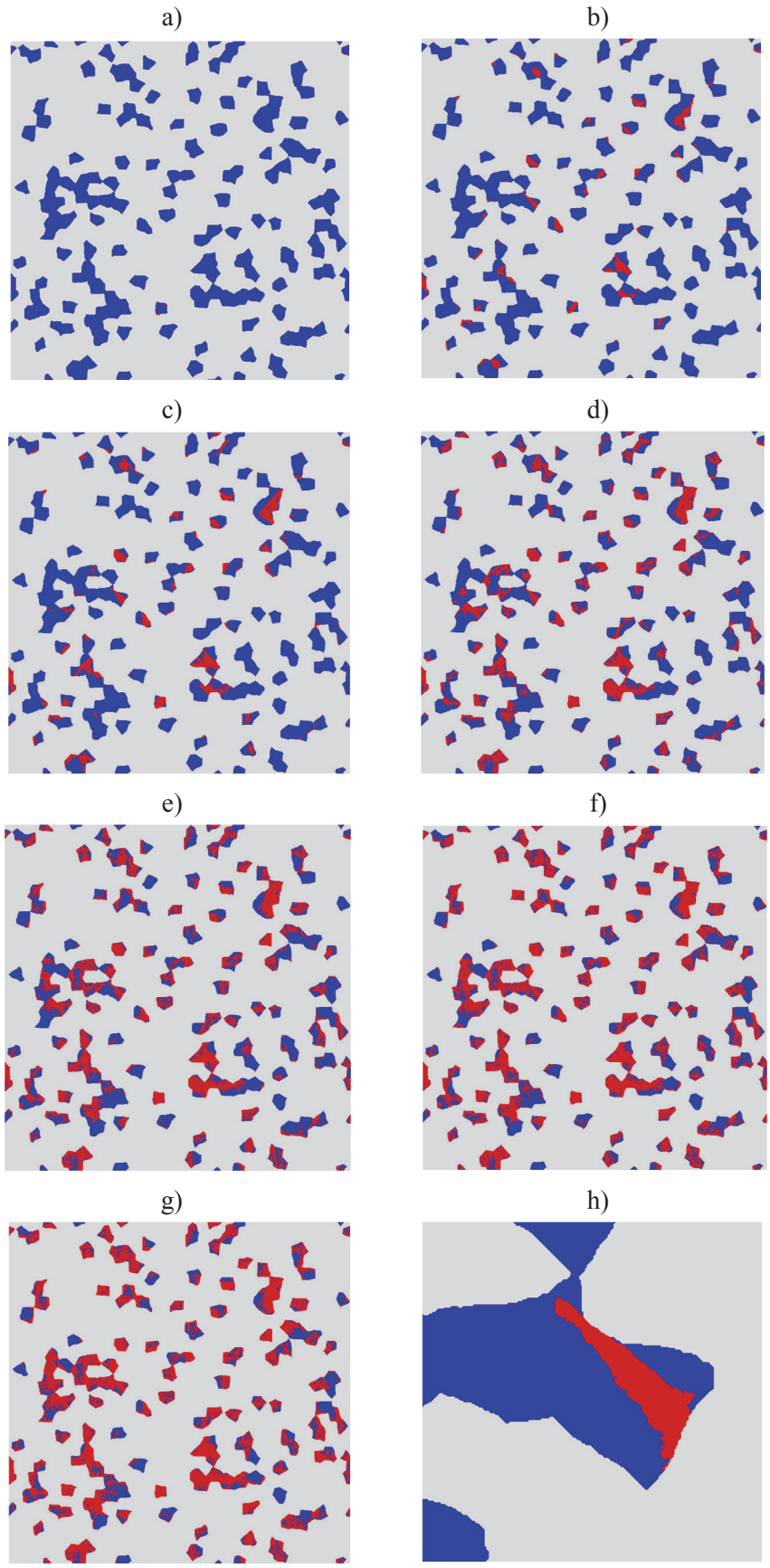

Fig. 9. *Calculated shapes of islands of retained austenite (blue) and martensite (red) in the RVE after the strain of 5E-06 (a), 6E-04 (b), 0.0036 (c), 0.016 (d), 0.0357 (e), 0.076 (f), and 0.12 (g), enlarged single martensite island, 12x12μm sample (h)*

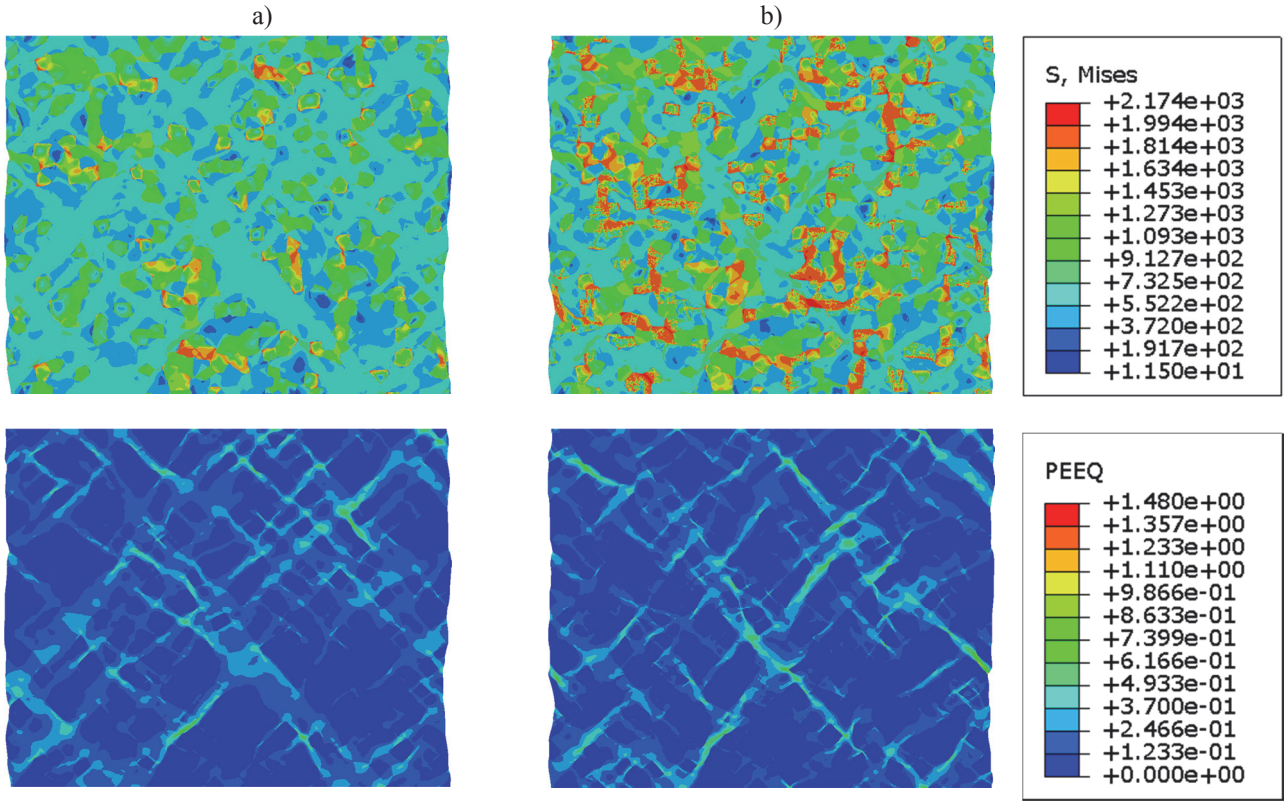

Fig. 10. *Effective stress distribution (top) and effective strain distribution (bottom) during RVE deformation without TRIP effect (a) and with TRIP effect (b).*

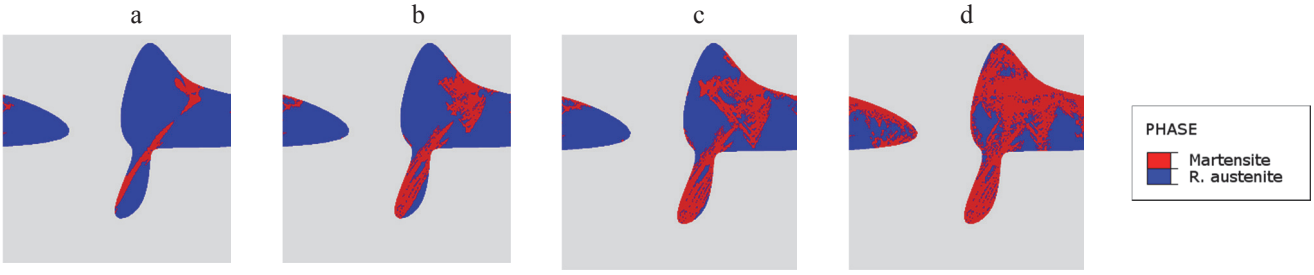

Fig. 11. *Calculated shapes of islands of retained austenite (blue) and martensite (red) in the SSRVE after the strain of 0.0202 (a), 0.017 (b), 0.03 (c), 0.38 (d).*

The strain-induced transformation effect has very well been studied for metastable austenite stainless steels and for TRIP steels, see for example (Murr, 1987). An empirical formula for the strain induced transformation effect in multiphase steel has been proposed in (Goel et al., 1985; Wiewiórowska, 2010. The mechanical stability of the austenite has been also studied by Ludwigson and Berger (1969) and the following experimentally found mathematical relation was used in this paper:

$$\frac{1}{F_{RA}} - \frac{1}{F_{RA0}} = \frac{A\varepsilon^{B}}{F_{RA0}} \tag{3}$$

where: F_{RA0}, F_{RA} – initial and current volume fraction of residual austenite in the TRIP steel microstructure, respectively, A – a constant representing the propensity to transform, B – the autocatalytic transformation index., ε – strain.

In publication (Wei et al., 2002) material parameters A and B in equation (3) were determined experimentally for very low strain rates and for dynamic conditions. In the present paper linear relation of A and B on logarithm of the strain rate was assumed and values obtained by Wei et al. (2002)were interpolated by the following functions of the strain rate:

$$\begin{aligned} A &= 9.697 + 1.5386 \lg\left(\dot{\varepsilon}\right) \\ B &= 0.775 + 0.05746 \lg\left(\dot{\varepsilon}\right) \end{aligned} \tag{4}$$

In order to validate this approach numerical simulations of deformation of the TRIP microstructure were performed. RVE with TRIP microstructure was developed first and was subjected to deformation by

compression to the strain of 0.15 with the average strain rate of 9.06×10^{-3} s^{-1}. In this approach the RVE with the microstructure shown in Fig. 8a containing 50% of ferrite (white), 20% of bainite (green), 10% of martensite (black) and 20% of retained austenite (red) was investigated. The size of the RVE was 1500×1500 μm. The fully coupled model was used. Results showing martensite and retained austenite at various stages of deformation are presented in Fig. 9.

Further numerical tests included simulation of the RVE shown in Fig. 8a accounting for the TRIP effect and neglecting it. Results of these simulations are presented in Fig. 10. It is seen that accounting for the TRIP effect has noticeable influence on stress and strain distribution in the deformation zone.

By using this methodology, simple, periodic unit cell, which reflects the behaviour of the source TRIP microstructure, was obtained (Fig. 8b). SSRVE cell was generated inside optimization procedure where selected features of source RVE image and artificial cell were compared. Non-uniform rational B-spline (NURBS) were used for grains representation due to proven high geometry modelling capabilities and low computational cost. Deformation of the statistically similar representative element with the TRIP microstructure was simulated and the results are presented in figure 11.

Computing times for different approaches were compared and the following results were obtained for the processor Intel Core i7 6700K when 8 Cores were used:

- RVE – without the TRIP effect: 1414 s
- RVE – with the TRIP effect: 15385 s
- SSRVE – with the TRIP effect: 1732 s

6. DISCUSSION OF RESULTS AND CONCLUSIONS

In the first approach the flow stress model for the investigated steels was determined on the basis of the inverse analysis for the compression tests. In order to analyse local material behaviour accounting for the TRIP effect, an attempt of simulation of the steel sample with the TRIP microstructure was performed. This microstructure was reproduces in the RVE and in the SSRVE. Motion of the interface between retained austenite and progressing martensite was simulated. The following conclusions were drawn on the basis of analysis of numerical results:

- Flow stress model developed on the basis of compression tests can be used for simulation of primary forming processes in the manufacturing chain for fasteners (drawing). Inverse analysis of the compression tests showed negligible sensitivity of the investigated steels to the strain rate and temperature.
- Accounting for the TRIP effect has an influence on the character of the local distribution of strains and stresses.
- Application of the statistically similar representative element allowed to decrease computing costs significantly.
- SSRVE with the TRIP microstructure, when attached to the FE code for simulation of finishing forming operations (eg. rolling of the thread), would be capable to predict local properties of the product accounting for the transformation of the retained austenite into martensite.

ACKNOWLEDGEMENTS

The work within the NCBiR project POIR.01.01.01-00-0033/15-00

REFERENCES

Balzani, D., Schroder, J., 2008, Some basic ideas for the reconstruction of statistically similar microstructures for multiscale simulations, *Proc. Appl. Math. Mech.*, 8, 0533-10534.

Bhadeshia, H.K.D.H., Christian, J.W., 1990, Bainite in steels, *Metallurgical Transactions A*, 21 767-797.

Cherkaoui, M., Berveiller, M., Lemoine, X., 2000, Coupling between plasticity and martensitic phase transformation: Overall behavior of polycrystalline TRIP steels, *International Journal of Plasticity*, 16, 1215-1241.

Davut, K., 2013, *Relation between microstructure and mechanical properties of a low-alloyed TRIP steel*, Materialwissenschaft, Shaker Verlag, Aachen.

Fonstein, N., 2015, TRIP Steels*, in: Advanced high strength sheet steels: Physical metallurgy, design, processing, and properties*, Springer, 185-239.

Furnemont, Q., Kempf, M., Jacques, P.J., Goken, M., 2002, On the measurement of the nanohardness of the constitutive phases of TRIP-assisted multiphase steels, *Materials Science and Engineering A*, 328 A, 26-32.

Goel, N.C., Sangal, S., Tangri, K., 1985, A Theoretical model for the flow behavior of commercial dual-phase steels containing metastable retained austenite: Part I. Derivation of flow curve equations, *Metallurgical Transactions A*, 16A, 2013-2029. 59.

Guo, L., Roelofs, H., Lembke, M.I., Bhadeshia, H.K.D.H., Modelling of size distribution of blocky retained austenite in Si-containing bainitic steels, *Materials Science and Technology*, 33, 2017, doi.org/10.1080/02670836.2017.1354797.

Hensel, A., Spittel, T., 1979, *Kraft- und Arbeitsbedarf Bildsamer Formgebungs-verfahren*, VEB Deutscher Verlag fur Grundstoffindustrie, Leipzig.

Iwamoto, T., Tsuta, T., Tomita, Y., 1998, Investigation on deformation model dependence of strain-induced martensitic transformation in TRIP steels and modelling of transformation kinetics, *International Journal of Mechanical Science*, 40, 173-182.

Konstantinov, D., Bzowski, K., Korchunov, A., Pesin, A., Pietrzyk, M., 2015, Multiscale modelling of ferritic-pearlitic steel deformation in rod drawing process by using statistical representation of microstructure, *Computer Methods in Materials Science*, 15, 336-345.

Kuziak, R., Kawalla, R., Waengler, S., 2008, Advanced high strength steels for automotive industry, *Archives of Civil and Mechanical Engineering*, 8, 103-117.

Ludwigson, D.C., Berger, J.A., 1969, Plastic behaviour of metastable austenitic stainless steels, *Journal of the Iron and Steel Institute*, 207, 63-69.

Murr, L.E., 1987, Metallurgical effects of shock and high-strain rate loading, in: *Materials at high strain rates*, (ed.) Blazynski, T.Z., Elsevier Applied Science Publishers Ltd., 1-46.

Papatriantafillou, I., Aravas, N., Haidemenopoulos, G.N., 2004, Finite element modelling of TRIP steels, *Steel Research International*, 75, 730-736.

Papatriantafillou, I., 2005, TRIP steels: constitutive modeling and computational issues, (Doctoral dissertation), Retrieved from University of Thessaly Institutional Repository, 77-82.

Perdahcioglu, E.S., Geijselaers, H.J.M., 2011, A model for TRIP steel constitutive behavior, *Proc. 14th Int. Conf. on Material Forming ESAFORM*, AIP Conference proceedings, Belfast, 1500-1504.

Perlade, A., Bouaziz, O., Furnemont, Q., A physically based model for TRIP-aided carbon steels behavior, Materials Science and Engineering, A356 (2003) 145-152.

Pietrzyk, M., Madej, Ł., Rauch, Ł., Szeliga, D., 2015, *Computational Materials Engineering: Achieving high accuracy and efficiency in metals processing simulations*, Elsevier, Amsterdam.

Rauch, Ł., Pernach, M., Bzowski, K., Pietrzyk, M., 2011, On application of shape coefficients to creation of the statistically similar representative element of DP steels, *Computer Methods in Materials Science*, 11, 531-541.

Schroeder, J., Balzani, D., Brands, D., 2011, Approximation of random microstructures by periodic statistically similar representative volume elements based on lineal-path functions, *Archives of Applied Mechanics*, 81, 975-997.

Szeliga, D., Gawąd, J., Pietrzyk, M., 2006, Inverse analysis for identification of rheological and friction models in metal forming, *Computer Methods in Applied Mechanics and Engineering*, 195, 6778-6798.

Wei, X.C., Li, L., Fu, R.Y., De Cooman, B.C., Wollants, P., Zhu, X.D., Wang, L., 2002, Influence of strain rate on strain-induced transformation of retained austenite to martensite in high strength low alloy TRIP steels, *Proc. Int. Conf. on TRIP-Aided High Strength Ferrous Alloys*, ed., De Cooman, B.C., Mainz, 373-378.

Wiewiórowska, S., 2010, The influence of strain rate and strain intensity on retained austenite content in structure of steel with TRIP Effect, *Solid State Phenomena*, 165, 216-220.

NUMERYCZNY MODEL ODKSZTAŁCENIA NA ZIMNO STALI TRIP

Streszczenie

Głównym celem artykułu było zbadanie możliwości modelowania odkształcenia stali TRIP w procesie wytwarzania elementów złącznych. W pierwszej kolejności wyznaczono zhomogenizowane naprężenie uplastyczniające badanych stali wykorzystując wyniki prób ściskania. W celu wyeliminowania wpływu tarcia i zamiany pracy odkształcenia na ciepło zastosowano analizę odwrotną. W drugiej części pracy badano możliwości przewidywania lokalnych odkształceń i naprężeń z uwzględnieniem efektu TRIP w stali. Skonstruowano reprezentatywny element objętości (REO) i statystycznie podobny reprezentatywny element objętości (SPREO) z mikrostrukturą TRIP. Te elementy zostały poddane odkształceniom w temperaturze otoczenia. W trakcie odkształcenia modelowano transformację austenitu szczątkowego w martenzyt. Porównano koszty obliczeń dla REO i SPREO i wykazano, że dla SPREO są one o rząd wielkości mniejsze. SPREO z mikrostrukturą TRIP, który może zostać zaimplementowany w modelu MES symulującym kucie elementów złącznych, jest głównym wynikiem pracy.

Received: December 20, 2017
Received in a revised form: January 31, 2018
Accepted: February 18, 2018